Journal of The Electrochemical Society, **148** (12) A1346-A1351 (2001)
0013-4651/2001/148(12)/A1346/6/$7.00 © The Electrochemical Society, Inc.

A Study of Copper as a Cathode Material for an Ambient Temperature Sodium Ion Battery

Sea H. Park,* Christopher W. Moore,* Paul A. Kohl,,z and Jack Winnick****

School of Chemical Engineering, Georgia Institute of Technology, Atlanta, Georgia 30332-0100, USA

The electrochemical behavior of copper was examined as a possible metal/metal(II) chloride cathode for a room temperature sodium battery in a nonaqueous melt comprised of methanesulfonyl chloride, aluminum chloride, and sodium chloride. Electrodes plated with a finite amount of copper showed a decrease in the amount of stored charge with increasing cycles, while solid copper electrodes showed a steady amount of oxidation and reduction. To keep the electrolyte buffered, the electrolyte contained excess NaCl in the form of a slurry. Results with a working electrode in NaCl slurry showed a Cu/Cu(II) coulombic efficiency (reduction/oxidation) of less than 100%, while a coulombic efficiency of 55% was observed for the electrode in the buffered slurry. On the other hand, a coulombic efficiency over 100% was observed for trials where the electrode surface was not submerged in the NaCl slurry resulting in a lower buffer capacity. This was probably due to local acidity change near the electrode surface caused by the decrease in chloride ions as the copper is oxidized to copper chloride. This local acidity may cause side reactions to take place that chemically participated in the oxidation. This was supported by results using an electrochemical quartz crystal nanobalance that show a greater increase in mass than expected from the amount of current passed during oxidation.
 [DOI: 10.1149/1.1413479]

Manuscript received March 1, 2001. Available electronically November 1, 2001.

The need for low-cost, dependable, high-energy density rechargeable batteries continues to escalate with the demands of the electronics and automobile industries. Use of a sodium-metal anode has been studied as an alternative to the lithium-based battery due to some potential advantages. Metallic lithium presents serious problems as an anode material in lithium-ion rechargeable batteries.[1] The formation of lithium dendrites during deposition has required the use of a separator and lowered the coulombic efficiency (stripping/plating).[2,3] A wide separation of these electrodes results in high resistance and low current density. Sodium-anode batteries, in contrast, can be constructed with a minimum of free electrolyte between electrodes because sodium deposits evenly on the surface of the electrode. Furthermore, sodium is inexpensive because of its abundant supply. These two factors may make sodium an attractive anode alternative.

One rechargeable sodium battery technology is the ''Zebra'' cell, which operates at ~250°C and uses a molten chloroaluminate inorganic salt, $NaCl:AlCl_3$, as the electrolyte.[4] At this temperature, the Zebra cell contains molten sodium (mp 98°C) as the anode, a solid separator, and a solid metal chloride (MCl_2) cathode. The half-cell and full-cell reactions are

	Charged	$\rightleftarrows$	Discharged
Anode	$2Na$	$\rightleftarrows$	$2Na^+ + 2e^-$
Cathode	$MCl_2 + 2e^-$	$\rightleftarrows$	$M + 2Cl^-$
Overall	$MCl_2 + 2Na$	$\rightleftarrows$	$2NaCl + M$

There are several advantages for a room temperature sodium cell. Along with decreasing the thermal management requirements, the sodium anode could operate in the solid state, thereby removing the need for the separator, and thus reducing the cell resistance. The use of sodium at or near room temperature demands an electrolyte that is low-melting, ionically conductive, and with an electrochemical window sufficiently large to permit both the deposition of sodium and a corresponding cathode reaction. One melt that has been shown to meet these qualifications is a mixture of methanesulfonyl chloride (MSC), aluminum chloride, and sodium chloride.[5,6]

Angell and others proposed molten salt electrolytes with an inorganic liquid salt replacing the organic salts.[6] The cathodic limit of many of these melts was 1 V negative of the sodium redox couple. The most attractive of these inorganic electrolytes was made from methanesulfonyl chloride, aluminum chloride, and a sodium salt ($N = 0.5$), where N is the mole fraction of aluminum chloride. The coulombic efficiency recorded for sodium or lithium couples in these electrolytes previously was between 50 and 90%, and the conductivity was $10^{-4.5}$ S/cm at 25°C.[6] The higher efficiency was only observed at slow scan rates, *ca*. 1.0 mV/s, and is probably due to the formation of a passivating film on the working electrode.[6] However, we were able to get 97% coulombic efficiency for sodium in the 35/65 MSC melt.[5]

Copper stability in lithium-ion electrolytes has also been studied because lithium-ion cells currently in production use a carbonaceous coating applied to a copper foil substrate as the negative electrode.[7,8] In some electrolytes, contaminants such as H_2O or HF may oxidize copper. Dissolution of copper should be avoided because the loss of copper on the cathode and/or the degradation of the melt will cause a decrease in performance with increasing cycles.

To be a suitable cathode material, copper must oxidize in the melt to form an insoluble metal chloride, remaining on the electrode, that can be reduced with a high coulombic efficiency (near 100%). It also must be stable in the melt and not oxidize at open-circuit potentials.

In this paper, an electrochemical quartz crystal nanobalance (EQCN) has been used to investigate reactions on the surface of copper electrode in the MSC melt. In particular, exploration of the regions of potential (and current) where the coulombic efficiencies are above or below unity is important for understanding the mechanism of the parasitic reaction. The EQCN can be used in controlled potential or current electrochemical experiments. The mass change can be obtained from the Sauerbrey equation[9-12]

$$\Delta f = -\frac{2 f_0^2 \Delta m}{A(\mu_q \rho_q)^{1/2}} \quad [1]$$

where Δf is the frequency shift, f_0 is the resonant frequency, Δm is the mass change, A is the piezoelectrically active area, μ_q is the shear modulus of the quartz crystal, and ρ_q is the density of the quartz crystal. The mass change of the quartz crystal is inversely proportional to frequency shift. Linearity of frequency change with respect to mass change was observed from this relationship up to a certain thickness of the deposited film.[9,10] Mass change can be related to charge passed according to Faraday's law

$$\frac{dm}{dt} = \frac{I \cdot MM}{F \cdot n} \quad [2]$$

* Electrochemical Society Student Member.
** Electrochemical Society Active Member.
z E-mail: paul.kohl@che.gatech.edu

where *MM* is the molecular mass, *n* is the number of equivalents per mole, and *F* is the Faraday constant.[9]

Experimental

All work was performed in a Vacuum Atmospheres Company inert atmospheric glove box in which H_2O and O_2 concentrations were maintained below 10 ppm. The electrochemical experiments were performed with an EG&G Princeton Applied Research model 273 potentiostat/galvanostat.

The experiments in the dry box were performed in a three-electrode glass cell. Working electrodes were made by electroplating copper from an aqueous solution of copper chloride onto 1.0 mm diam platinum wire (99.999%, ESPI, Ward Hill, MA). Solid copper electrodes were 2.0 mm diam copper wire (99.99%, ESPI). Nickel, iron, palladium, aluminum, and tungsten wires from ESPI were also used as electrodes. The counter electrodes were coiled platinum wires. The reference electrode was a 0.5 mm diam aluminum (99.999%, Alfa, Ashland, OR) wire immersed in an acidic MPIC melt (0.6 mol of aluminum chloride and 0.4 mol of methyl-propyl imidazolium chloride) contained in a fritted borosilicate glass tube.

Methanesulfonyl chloride (99%), aluminum chloride, and sodium chloride (99.999%) were obtained from Aldrich Chemical (Milwaukee, WI). The melt was prepared by adding small increments of aluminum chloride to MSC. The final molar ratio of MSC to $AlCl_3$ was 65:35; the melt was then saturated with excess NaCl to ensure that it was buffered with NaCl. Before the addition of NaCl, the melt is light yellow; after it becomes saturated with NaCl, the melt is clear in color and translucent.

An EQCN, model EQCN-701, from Elchema (New York, NY) was used in the melts to measure the mass change on a quartz crystal. The working electrode in these experiments was either a 10 MHz AT-cut platinum-coated or gold-coated quartz crystal from ICM (Oklahoma City, OK). These crystals were electroplated or sputtered with copper. The EQCN cell was operated in a Faraday cage to minimize the electrical noise. A potentiostat, EG&G bio366 was used with an EG&G 175 universal programmer and HP 7090A plotter. The EQCN was calibrated for charge-to-mass measurements by electroplating copper from an acidic, aqueous copper sulfate solution. A duplicate calibration was performed by depositing silver from an acidic silver nitrate solution. The potential of the quartz crystal electrode was cycled to values negative of the deposition potential; the mass change and charge were recorded. The potential of the quartz crystal working electrode was scanned positive of the deposition potential to strip the copper (or silver) from the surface and the mass returned to its original value.

Results and Discussion

Figure 1 shows a cyclic voltammetry (CV) scan of a platinum working electrode in the 35/65 MSC melt. The scan begins in the positive direction from the open circuit voltage. As the potential moves positive of 2.0 V, oxidation of chloride ions in the melt takes place, producing chlorine gas. The platinum is not oxidized at these potentials. This shows the background for the MSC melt at the positive end of its electrochemical window.

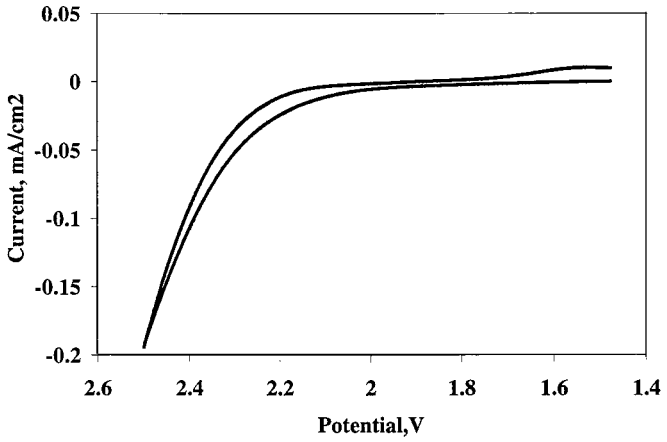

Figure 1. CV of platinum in 35/65 MSC melt showing the positive end of electrochemical window of melt.

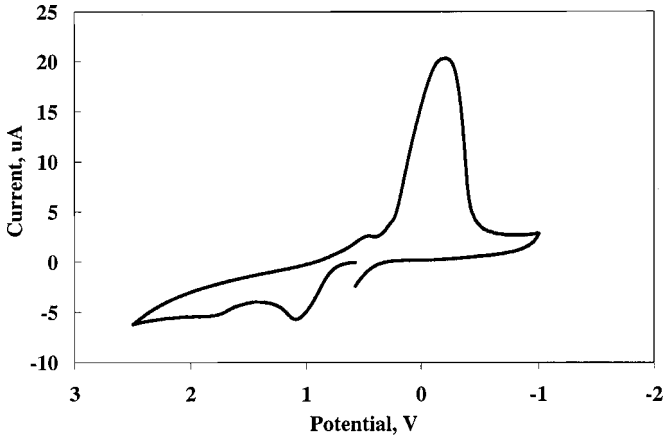

Figure 2. CV of Cu in 35/65 MSC melt. Scan started in the positive direction showing oxidation then reduction. Electrode area is 0.0079 cm^2.

Figure 2 and 3 show voltammograms for a copper working electrode in the 35/65 MSC melt. Figure 2 begins with a positive scan showing the copper being oxidized when the potential is positive of 1.0 V

$$Cu + Cl^- \rightleftarrows CuCl + e^- \quad [3]$$

or

$$Cu + 2Cl^- \rightleftarrows CuCl_2 + 2e^- \quad [3]$$

Upon scan reversal, a reduction current is observed when the potential is negative of initial starting potential. Figure 3 is a scan started in the negative direction. No current is observed in the potential range corresponding to the reduction peak in Fig. 2. This shows that the reduction peak in Fig. 2 is a result of the copper oxidation process. The oxidation products, which were insoluble, remained on the electrode surface. The number of coulombs observed for the oxidation was often less than that for the reduction, as can be seen from the anodic and cathodic areas in Fig. 2. The cause of this unusual result was investigated, as described below.

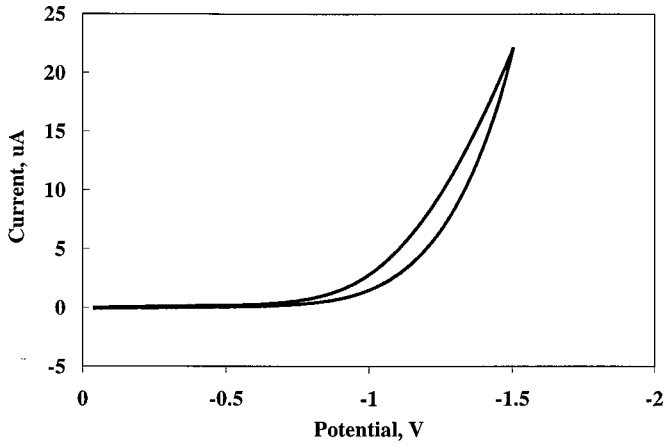

Figure 3. CV of Cu in 35/65 MSC melt. The scan started in the negative direction showing no reduction. Electrode area is 0.0079 cm^2.

Figure 4 and 5 are examples of chronoamperommetry (CA) experiments for copper-plated electrodes in the 35/65 MSC melt. The CAs show an oxidation and reduction of copper when held at constant potential. The potentials used were 0.9 and 0.3 V for oxidation and reduction, respectively. However, the environment of the working electrode was varied from typical in solution (Fig. 4) to submerged in the NaCl slurry (Fig. 5). This slurry of NaCl is more likely to maintain the chloride buffering at the working electrode. The behavior of copper during oxidation/reduction may thus be different in the slurry from that in the solution.

Figure 4 shows results from the CA for the copper-plated electrode in the supernatant above the NaCl slurry. The first and tenth scans were plotted for comparison. The first noticeable difference between these scans was a higher magnitude of oxidation/reduction peak currents in the first scan. This difference is also apparent when the total charge transferred during each scan was compared. For an example, oxidation and reduction coulombs for the first run are approximately three times greater than for the tenth run; coulombic efficiencies for the first and tenth scans are 147 and 169%, respectively. Greater than 100% coulombic efficiencies suggest possible parasitic reactions with oxidized species (copper chloride) or reduction of impurities.

CA experiments with the same 35/65 MSC melt as above, utilized a copper-plated platinum electrode submerged in the NaCl slurry as a working electrode; the results are shown in Fig. 5. Differences between oxidation and reduction peak currents for the first and tenth runs were minimal. For an example, coulombic efficiencies for the first and tenth scans were 56 and 54%, respectively.

Figure 6 shows results from the first ten CAs in the 35/65 MSC melt with a copper-plated electrode submerged in the NaCl slurry. Oxidation and reduction coulombs decreased slightly as the number of runs increased. Coulombic efficiencies for the first ten scans varied only slightly and were less than 100%. A possible cause of low coulombic efficiency is physical severance of some CuCl by reduction of an underlayer of CuCl. Declining oxidation coulombs with each sequential run indicates that changes were made at the surface of the electrode or electrolyte. One possible explanation is loss of copper from the substrate (platinum wire) in the form of CuCl, and decrease in available copper metal for oxidation as the CA experiment continued. The color of the electrode returned to that of Pt after many exhaustive tests; this fact supports the loss of the plated copper.

Results obtained with the copper-plated electrode in the supernatant above the NaCl slurry was examined for comparison with the copper electrode in the slurry. As explained earlier for this working electrode, reduction coulombs were greater than oxidation coulombs; these results are shown in Fig. 7. Coulombic efficiencies for copper reduction/oxidation escalated with sequential runs and were well over 100%. Many possible reasons were suggested to explain the coulombic efficiencies greater than 100%. Starting with chemical components in the electrolyte, there are sodium (Na^+), chloride (Cl^-), NaCl, methanesulfonyl ions (MS^+), tetrachloroaluminate ($AlCl_4^-$), and unknown impurities including H^+. Electrochemical reduction of these components has been considered to contribute higher coulombic efficiencies. Co-reduction of Na^+/MS^+ was considered but ruled out because their reduction potentials are far too negative, *i.e.*, −2.4 V.[5] The reduction potential for copper chloride

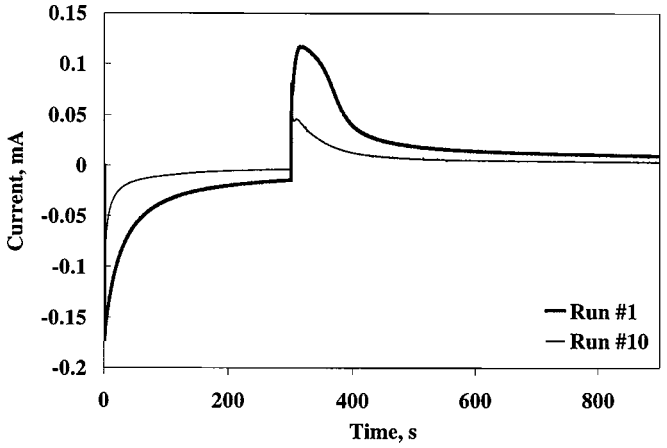

Figure 4. CA of a copper-plated electrode submerged in supernatant above NaCl slurry. Electrode area is 0.158 cm^2.

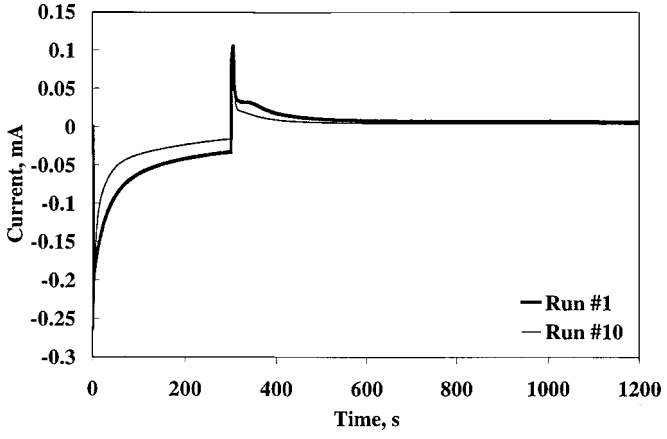

Figure 5. CA of a copper-plated electrode submerged in NaCl slurry. Electrode area is 0.158 cm^2.

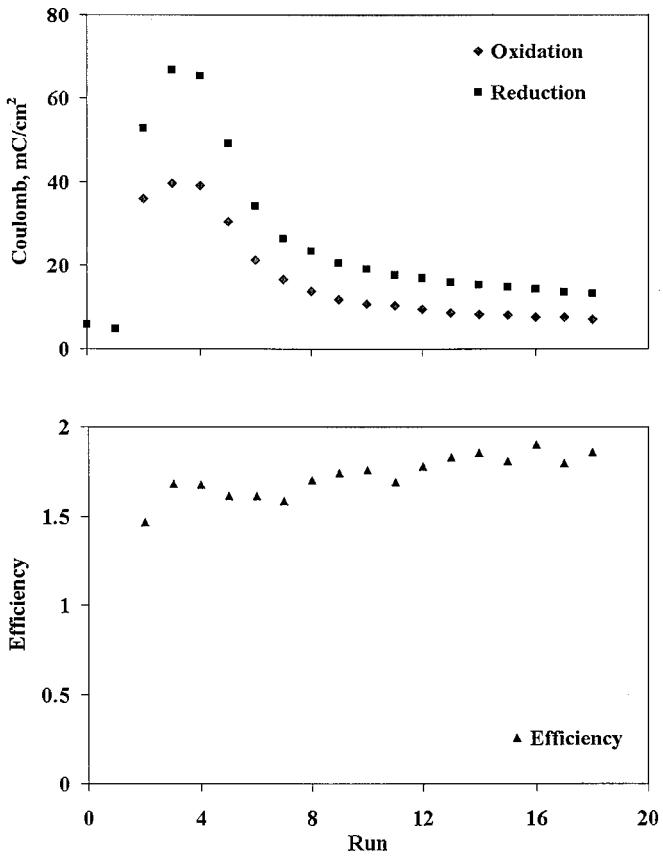

Figure 6. Plot of CA results of copper-plated electrode in slurry showing less reduction than oxidation.

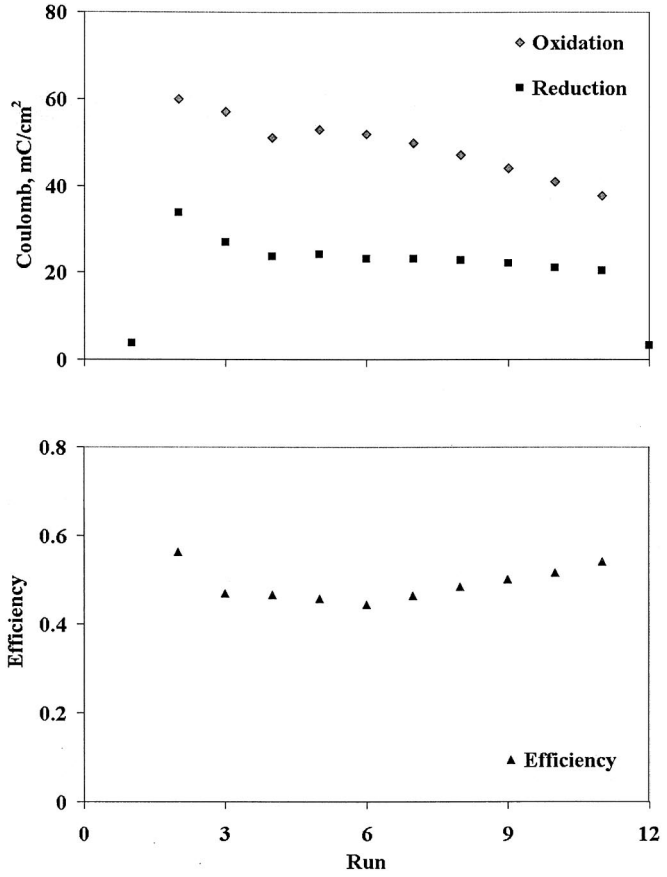

Figure 7. Plot of CA results of copper-plated electrode in supernatant above NaCl slurry showing more reduction than oxidation.

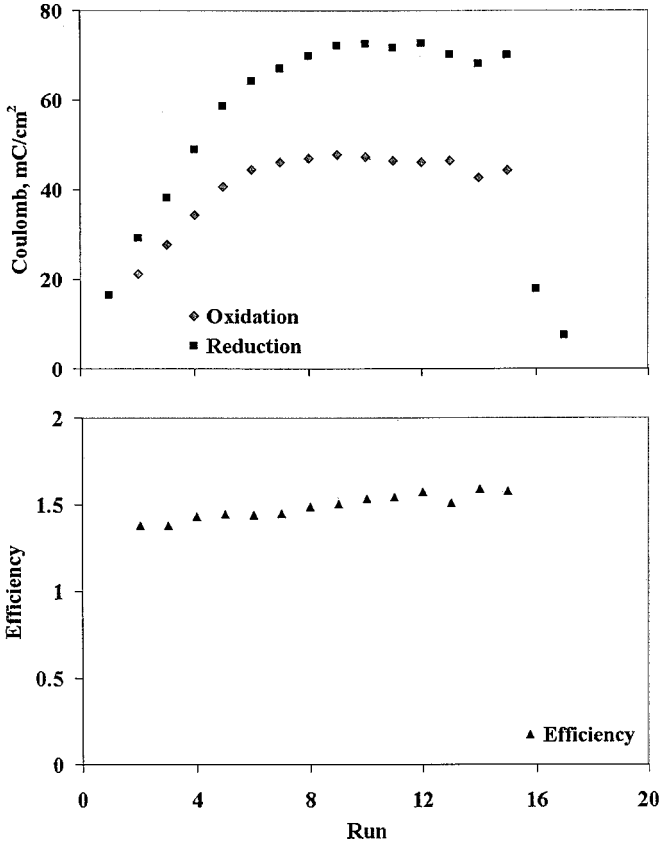

Figure 8. Plot of CA results of solid copper electrode with steady oxidation and reduction.

is +0.2 V. Electrochemical reduction of $AlCl_4^-$ to Al did not occur in the absence of Cu (*e.g.* Fig. 3).

$$AlCl_4^- + 3e \rightarrow Al + 4Cl^-$$

Reduction of H^+ could also be ruled out because there was no noticeable reduction current observed at +0.2 V in Fig. 3. Therefore, electroreduction of these chemical components could not contribute to the reduction current and result in greater than 100% coulombic efficiencies.

Parasitic chemical reactions were considered next as possible causes for coulombic efficiencies in excess of 100% and would be the most probable cause to explain this behavior, for example:

$$3Cu + Al_2Cl_7^- \rightarrow Al + AlCl_4^- + 3CuCl \quad [4]$$

$$3CuCl + Al_2Cl_7^- \rightarrow Al + AlCl_4^- + 3CuCl_2 \quad [5]$$

$$CuCl + Al_2Cl_7^- + Cu \rightarrow Al + AlCl_4^- + 2CuCl_2 \quad [6]$$

Depletion of local chloride concentration due to oxidation of copper will shift the equilibrium from $AlCl_4^-$ toward $Al_2Cl_7^-$. Products from this equilibrium shift are metallic aluminum and chloride ions. The aluminum may plate on the electrode, with some of the CuCl oxidizing to $CuCl_2$. During the negative-going scan, each plated $CuCl_2$ was reduced with two electrons. This should result in 200% coulombic efficiency in the ideal case, but in reality not all the CuCl was chemically oxidized to $CuCl_2$. Further, some of the $CuCl_2$ may be detached from the electrode during reduction of the underlying layers. This explains the declining coulombs for both oxidation and reduction with sequential runs. As copper on the substrate was lost in a form of copper chloride, the amount of copper available for oxidation dropped, and the oxidation and reduction coulombs decreased.

The composition of this electrolyte also supports the fact that parasitic reactions would be the main causes of the additional reduction charge. The high concentration of $AlCl_4^-$ would provide a high number of $Al_2Cl_7^-$ ions for these possible reactions. The reduction charge in Fig. 7 is almost 50% larger than the oxidation charge. To have this much charge, a high concentration of the oxidizing agent is required, and $AlCl_4^-$ fulfills this adequately. In the NaCl slurry, the

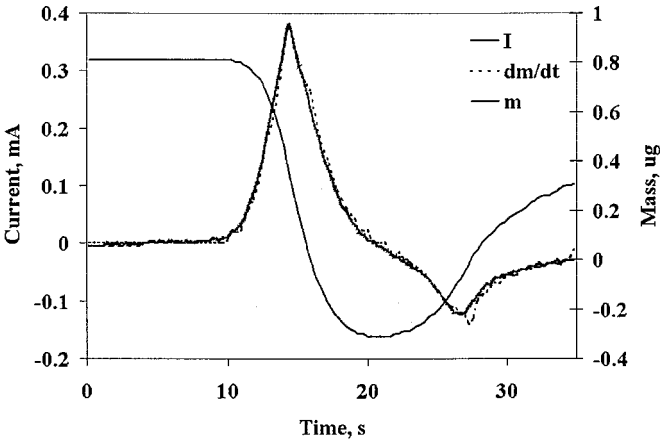

Figure 9. CV of copper-plated Pt quartz crystal using the EQCN. Electrode area is 0.196 cm^2.

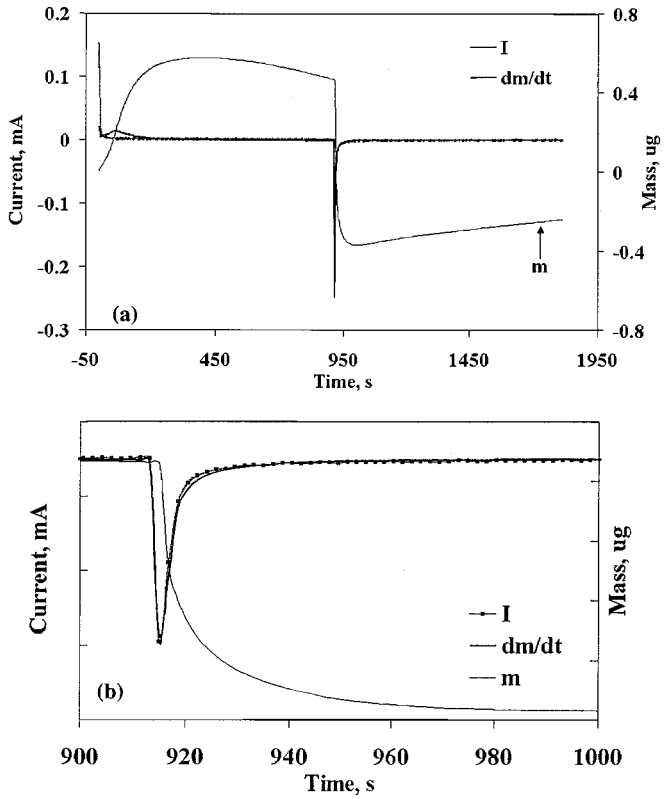

Figure 10. (a, top) CA of copper-plated Pt quartz crystal using the EQCN. (b, bottom) Shows the first 100 s of reduction step. Electrode area is 0.196 cm^2.

Cl^- concentration at the working electrode remains high, eliminating these reactions.

A solid copper electrode was incorporated into the CA experiments to test the previous proposition of the loss of copper; the results are plotted in Fig. 8. In the 35/65 MSC melt, coulombic efficiencies greater than 100% were observed. Unlike the copper-plated electrode, oxidation and reduction coulombs increased with each sequential run. This is due to the abundant accessibility of new copper (for these experiments) and the changes in the working electrode surface caused by reduction of copper chloride and its severance from the electrode. After the sixth run, the oxidation/reduction coulombs leveled off and became constant as the scan number increased.

An EQCN was used to examine the mass of the material plated on the copper electrode. The 35/65 melt MSC was diluted to 27:73 of $AlCl_3$ and methanesulfonyl chloride for the EQCN experiments to overcome the damping problem with quartz crystals in viscous ionic solutions. A voltage scan with the EQCN is shown in Fig. 9, in which current and mass are plotted *vs.* time. The rate of the change of mass with time (dm/dt) is also plotted. For the ideal reversible system, dm/dt should exactly overlap the current (I) according to Faraday's law, Eq. 2. The scan started at 0.6 V, swept at a rate of 100 mV/s to 2.0 V, then swept back to 0.6 V.

The approximate molecular mass (MM/N) to charge ratio was calculated (Eq. 2), using the total mass change and current, to be equal to 70 during oxidation. Figure 9 shows that dm/dt closely overlays the current throughout the scan, but the final mass did not return to its initial value. A sharp rise of current and dm/dt at the 10 s mark is probably due to the electrochemical oxidation of copper on the working electrode with chloride ions to form CuCl. This oxidation process would require one electron for each chloride ion, with a corresponding molecular mass of 35. However, the actual MM/N of 70 was approximately twice that. This higher MM/N indicates chemical reactions occur between the oxidized product (*i.e.*, CuCl) and the melt, or the oxidized product was not CuCl or $CuCl_2$. Since the oxidation product was insoluble and could be reduced, the former explanation was favored. As proposed earlier, CuCl was chemically oxidized to $CuCl_2$, and the reaction rate of this conversion was relatively fast giving a MM/N of 70 instead of 35. This result agrees with CV and CA results described previously for the copper-plated platinum wire electrode.

Reduction currents for copper chloride started to rise at the 20 s point on the x axis while mass started to decrease. The slope, dm/dt, overlays the reduction current using 72 as MM; this near-match indicated that mass change was mainly due to an electrochemical reduction. However, it is rather difficult to rationalize that the reduced product has a molecular mass-to-charge of 72. One explanation for this high molecular mass is that chemical reactions occurring during oxidation can be reversed as the chloride concentration increases. Other possibilities include dissolution of CuCl or $CuCl_2$ from the electrode as chloride ion is released, or loss of mass from the electrode due to adhesion problems. The dissolution of copper compounds would result in a loss of oxidation coulombs with sequential runs, and eventually no copper would remain on the working electrode.

The results from the exhaustive CA scan with the EQCN are shown in Fig. 10. Copper was electroplated on a Pt quartz crystal as a working electrode. The oxidation potential was 1.3 V, and the reduction potential was 0.4 V; each potential was held for 900 s. The MM was calculated to be approximately 33 for the oxidation and 50 for the reduction. These values are close to those expected for chloride participation (*i.e.*, 35). The coulombic efficiency for copper redox was 101%, and the mass efficiency was 152%. The magnitude of the reduction and oxidation currents was relatively low compared to the other experiments; the current density is only one tenth of the results in Fig. 6, 7, and 8. A mass of 0.46 μg of oxidized species deposited during the oxidation process, and 0.7 μg was stripped during the reduction step. However, low redox currents suggest that depletion of Cl^- ions would be small and result in no significant change of acidity in the vicinity of a working electrode. This would also lower the possibility of chemical reactions due to the lack of an equilibrium shift from $AlCl_4^-$ toward $Al_2Cl_7^-$. Parasitic reactions would not occur during this exhaustive CA scan.[5-7]

The MM for the first 100 s of reduction was calculated to be 77. The inset in Fig. 10 shows the first 100 s of the reduction step. A sharp drop in mass is observed as the potential is switched from oxidation to reduction. The slope, dm/dt, again closely overlayed the current. This agreement confirms that most of the mass stripped was due to the reduction current, and the high MM is explained by chemical and electrochemical removal of chloride. These results are further evidence for reversible chemical reactions occurring during oxidation and reduction steps, as explained earlier.

As seen in Fig. 10, electrode mass was starting to decrease after 400 s of oxidation, though the current had dropped to near zero. This decline would be caused by physical loss of copper chloride ($CuCl_2$). The adherence of $CuCl_2$ to the electrode in the MSC melt is believed to be inferior to that of CuCl. This weakness of $CuCl_2$ might also cause $CuCl_2$ detachment during the reduction step. The mass increases from the 100 s point of reduction until termination of the scan. This rising mass is explained by the reduction current observed during a background current scan with a pure platinum electrode. The low molecular mass during this rising current region is due to electrodeposition from the melt of copper, aluminum, or both. A deposited layer of aluminum or Al-Cu alloys will lessen oxidation coulombs for the next scans as the area of copper metal exposed to the electrolyte decreases.

Greater than 100% coulombic efficiencies and the high oxidation molecular mass from the EQCN experiments are indicators of side reactions. We suspect that as copper is oxidized to CuCl, the equilibrium between $AlCl_4$ and $Al_2Cl_7^-$ shifts in the direction of

$Al_2Cl_7^-$. The copper can then be further chemically oxidized in this locally acidic solution.

Conclusions

Results from cyclic voltammetry, chronoamperommetry, and electrochemical quartz crystal microbalance experiments show that copper oxidizes and reduces near the positive end of the electrochemical window for the 35:65 $AlCl_3$:MSC melt. Local acidity in the melt will cause unwanted side reactions, but can be reduced or prevented when buffered in a slurry of NaCl. Thus, copper may be a viable cathode in a room-temperature sodium battery, but careful control of the electrolyte is necessary.

Acknowledgments

This project was supported by the U.S. Department of Energy, Basic Energy Science, under grant no. DE-FG02-97ER14798. In particular, Dr. Paul Maupin, Program Manager, is gratefully acknowledged for his support and encouragement. We also acknowledge Professor C. A. Angell and his research group, Department of Chemistry, Arizona State University, for their technical assistance with methanesulfonyl chloride melts.

The Georgia Institute of Technology assisted in meeting the publication costs of this article.

References

1. T. Piao, S.-M. Park, C.-H. Doh, and S.-I. Moon, *J. Electrochem. Soc.*, **146**, 2794 (1999).
2. J. O. Besenhard, *Handbook of Battery Materials*, Wiley-VCH, Weinheim (1999).
3. I. Yoshimatsu, T. Hirai, and J.-i. Yamaki, *J. Electrochem. Soc.*, **135**, 2422 (1988).
4. R. J. Bones, J. Coetzer, R. C. Galloway, and D. A. Teagle, *J. Electrochem. Soc.*, **134**, 2379 (1987).
5. S. H. Park, J. Winnick, and P. A. Kohl, *J. Electrochem. Soc.*, **148**, A346 (2001).
6. K. Xu, S. Zhang, and C. A. Angell, *J. Electrochem. Soc.*, **143**, 3548 (1996).
7. D. Aurbach and Y. Cohen, *J. Electrochem. Soc.*, **144**, 3355 (1997).
8. M. Zhao, S. Kariuki, H. D. Dewald, F. R. Lemke, R. Staniewicz, E. J. Plichta, and R. A. Marsh, *J. Electrochem. Soc.*, **147**, 2874 (2000).
9. Z. Lin, C. M. Yip, I. S. Joseph, and M. D. Ward, *Anal. Chem.*, **65**, 1546 (1993).
10. K. K. Kanazawa and O. R. Melroy, *IBM J. Res. Dev.*, **37**, 157 (1993).
11. J. Rickert and A. Brecht, *Anal. Chem.*, **69**, 1441 (1997).
12. M. Urbakh and L. Daikhin, *Colloids Surf., A,* **134**, 75 (1998).